



European Coordination for Accelerator Research and Development

PUBLICATION

A Concatenation Scheme for the Computation of Beam Excited Higher Order Mode Port Signals

Flisgen, T (University of Rostock) *et al*

04 June 2013

The research leading to these results has received funding from the European Commission under the FP7 Research Infrastructures project EuCARD, grant agreement no. 227579.

This work is part of EuCARD Work Package **10: SC RF technology for higher intensity proton accelerators and higher energy electron linacs.**

The electronic version of this EuCARD Publication is available via the EuCARD web site <<http://cern.ch/eucard>> or on the CERN Document Server at the following URL : <<http://cds.cern.ch/record/1553214>>

A CONCATENATION SCHEME FOR THE COMPUTATION OF BEAM EXCITED HIGHER ORDER MODE PORT SIGNALS

T. Flisgen*, H.-W. Glock†, U. van Rienen, Universität Rostock, IEF, IAE, Germany

Abstract

Ongoing studies [1, 2] investigate in how far higher order mode (HOM) port signals of superconducting RF cavities can be used for machine and beam diagnostics. Apart from experiments e.g. at the FLASH facility at DESY in Hamburg, numerical modelling is needed for the prediction of HOM coupler signals. For this purpose, the RF properties of the entire accelerating module have to be taken into account, since higher order modes can propagate along the cavity chain. A discretization of the full chain, followed by a wake field simulation is only feasible with powerful and expensive cluster computers. Instead, an element-wise wake field simulation of subsections of the chain, followed by a suitable concatenation scheme can be performed on standard hardware assuming the beam to be sufficiently stiff. In this paper a concatenation scheme for the computation of beam excited HOM port signals is derived as a generalization of the Coupled S-Parameter scheme CSC [3]. Furthermore, the validity of the method is shown for a sample structure.

INTRODUCTION

Running investigations [1, 2] on beam excited higher order mode (HOM) port signals of the module ACC39, mounted in the free-electron laser FLASH/DESY, evaluate the usability of these signals for diagnostic purposes. Beside of measurements of the HOM port signals with fast oscilloscopes and spectrum analyzers, computer simulations are essential to understand the excitation process and the dependency of the shape of the HOM signals on beam and machine parameters.

The characterization [4] of ACC39 has shown that higher order modes are not localized in the individual cavities, but are able to propagate through the entire chain of four cavities, incorporated by ACC39. The calculation of beam driven port signals of such large and complex structures is a computationally expensive task, which may be tackled by using massive parallel computer codes in combination with cluster computers (see e.g. [5]). As an alternative, complex accelerating structures can be decomposed into segments. The beam excited port signals of the segments are computed individually by means of transient wake field solvers and are concatenated by the presented scheme to obtain the beam driven port signals of the full structure.

THE CONCATENATION SCHEME

The proposed method, which is denoted as Coupled Transient Calculations (CTC), generalizes the well-established CSC method [3]. In comparison to CSC, the CTC formalism allows for segments having internal sources e.g. field exciting beams of charged particles traversing these segments. Note, that the presented concatenation scheme is restricted to excitation problems, where the beam is stiff such that field equations and equations of motion are decoupled. Furthermore, the structure under consideration has to be made of linear materials.

Splitting and Description of Segments

The first step is the splitting of the full structure into smaller segments, whose numerical treatment is less computationally demanding (see example in Fig. 1). In princi-

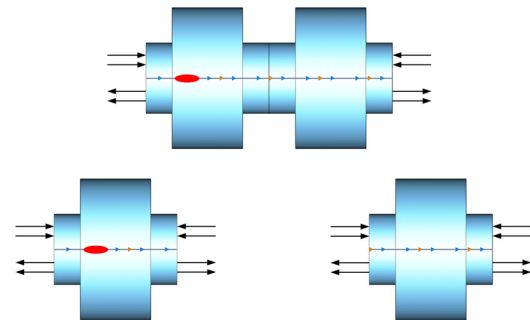


Figure 1: Splitting of a system of two coupled cylindrical cavities with schematic beam (red) and incident and scattered waves at matched waveguide ports (black arrows).

ple, on the cut planes an infinite number of waveguide port modes has to be considered for the orthogonal expansion. However, if the frequency interval on which the structure is examined is finite, it is sufficient to consider a finite number of port modes. It is favourable to split the structure at regions of constant cross section to reduce the number of port modes, required for the expansion. The signals scattered in the waveguide port modes of the k -th segment, denoted in frequency domain as $\vec{b}_k(s)$ can be expressed as

$$\vec{b}_k(s) = \mathbf{S}_k(s) \vec{a}_k(s) + \vec{y}_k(s). \quad (1)$$

Here $s = j\omega$ specifies the angular frequency and $\mathbf{S}_k(s)$ the scattering matrix. $\vec{a}_k(s)$ are the amplitudes of the waves which are incident to the waveguide ports. $\vec{y}_k(s)$ denotes the beam driven signals scattered in the waveguide ports, presuming the waves $\vec{a}_k(s)$ which are incident to the waveguide ports of the segment to be zero. All quantities are complex and refer to the k -th element.

05 Beam Dynamics and Electromagnetic Fields

D06 Code Developments and Simulation Techniques

* Thomas.Flisgen@Uni-Rostock.de

† Work funded by EU FP7 Research Infrastructure Grant No. 227579

Coupling of Subsections

For the sake of coupling of the subsections, the ansatz Eq. 1 is expressed for all N segments as the block system

$$\vec{b}_{can}(s) = \mathbf{S}_{tot}(s) \vec{a}_{can}(s) + \vec{y}_{can}(s), \text{ where} \quad (2)$$

$$\vec{b}_{can}(s) = \begin{pmatrix} \vec{b}_1(s) \\ \vdots \\ \vec{b}_N(s) \end{pmatrix}, \quad (3)$$

$$\mathbf{S}_{tot}(s) = \begin{pmatrix} \mathbf{S}_1(s) & \mathbf{0} & \dots & \mathbf{0} \\ \mathbf{0} & \mathbf{S}_2(s) & \dots & \mathbf{0} \\ \vdots & \vdots & \ddots & \vdots \\ \mathbf{0} & \mathbf{0} & \dots & \mathbf{S}_N(s) \end{pmatrix}, \quad (4)$$

$$\vec{a}_{can}(s) = \begin{pmatrix} \vec{a}_1(s) \\ \vdots \\ \vec{a}_N(s) \end{pmatrix}, \vec{y}_{can}(s) = \begin{pmatrix} \vec{y}_1(s) \\ \vdots \\ \vec{y}_N(s) \end{pmatrix}. \quad (5)$$

The described ordering of the signals is declared as canonical ordering. In a next step, a permutation matrix \mathbf{P} is used to sort the signals such that all m internal quantities and all n external quantities are separated:

$$\vec{b}_{sort}(s) = \begin{pmatrix} \vec{b}_{int}(s) \\ \vec{b}_{sct}(s) \end{pmatrix} = \mathbf{P} \vec{b}_{can}(s). \quad (6)$$

Internal quantities belong to ports of segments which are connected to other ports of other segments, whereas external quantities belong to ports which are not connected to other ports internally. Analog to Eq. 6 it holds that $\vec{a}_{sort}(s) = \mathbf{P} \vec{a}_{can}(s)$ and $\vec{y}_{sort}(s) = \mathbf{P} \vec{y}_{can}(s)$. Exploiting the orthogonality of the permutation matrix $\mathbf{P}^T = \mathbf{P}^{-1}$ and replacing the canonical quantities in Eq. 2 by the sorted quantities yields

$$\begin{pmatrix} \vec{b}_{int}(s) \\ \vec{b}_{sct}(s) \end{pmatrix} = \mathbf{P}^T \mathbf{S}_{tot}(s) \mathbf{P} \begin{pmatrix} \vec{a}_{int}(s) \\ \vec{a}_{inc}(s) \end{pmatrix} + \begin{pmatrix} \vec{y}_{int}(s) \\ \vec{y}_{sct}(s) \end{pmatrix}. \quad (7)$$

In a further step, a permutation matrix $\mathbf{A} \in \mathbb{R}^{m \times m}$ is used to express that the internal scattered quantities $\vec{b}_{int}(s)$ are fed back to the internal incident quantities $\vec{a}_{int}(s)$. The feedback is formulated by

$$\vec{a}_{int}(s) = \mathbf{A} \vec{b}_{int}(s). \quad (8)$$

Using the above statement, the vector containing the incident quantities in Eq. 7 can be expressed as

$$\begin{pmatrix} \vec{a}_{int}(s) \\ \vec{a}_{inc}(s) \end{pmatrix} = \underbrace{\begin{pmatrix} \mathbf{A} & \mathbf{0} \\ \mathbf{0} & \mathbf{I} \end{pmatrix}}_{\mathbf{F}} \begin{pmatrix} \vec{b}_{int}(s) \\ \vec{a}_{inc}(s) \end{pmatrix}, \quad (9)$$

where $\mathbf{I} \in \mathbb{R}^{n \times n}$ is the n -dimensional identity matrix.

Inserting Eq. 9 in Eq. 7 gives

$$\begin{pmatrix} \vec{b}_{int}(s) \\ \vec{b}_{sct}(s) \end{pmatrix} = \underbrace{\mathbf{P}^T \mathbf{S}_{tot}(s) \mathbf{P} \mathbf{F}}_{\mathbf{G}(s)} \begin{pmatrix} \vec{b}_{int}(s) \\ \vec{a}_{inc}(s) \end{pmatrix} + \begin{pmatrix} \vec{y}_{int}(s) \\ \vec{y}_{sct}(s) \end{pmatrix} \quad (10)$$

and expressing $\mathbf{G}(s)$ as a block matrix leads to

$$\begin{pmatrix} \vec{b}_{int}(s) \\ \vec{b}_{sct}(s) \end{pmatrix} = \begin{pmatrix} \mathbf{G}_{11}(s) & \mathbf{G}_{12}(s) \\ \mathbf{G}_{21}(s) & \mathbf{G}_{22}(s) \end{pmatrix} \begin{pmatrix} \vec{b}_{int}(s) \\ \vec{a}_{inc}(s) \end{pmatrix} + \begin{pmatrix} \vec{y}_{int}(s) \\ \vec{y}_{sct}(s) \end{pmatrix}. \quad (11)$$

It is highlighted that the dimensions of the block matrices correspond to the lengths m and n of the signal vectors:

$$\begin{aligned} \mathbf{G}_{11}(s) &\in \mathbb{C}^{m \times m}, & \mathbf{G}_{12}(s) &\in \mathbb{C}^{m \times n}, \\ \mathbf{G}_{21}(s) &\in \mathbb{C}^{n \times m}, & \mathbf{G}_{22}(s) &\in \mathbb{C}^{n \times n}. \end{aligned}$$

Taking the first row of Eq. 11 and solving for $\vec{b}_{int}(s)$ yields

$$\vec{b}_{int}(s) = [\mathbf{I} - \mathbf{G}_{11}(s)]^{-1} [\mathbf{G}_{12}(s) \vec{a}_{inc}(s) + \vec{y}_{int}(s)]. \quad (12)$$

Subsequently, taking the second row of Eq. 11 gives

$$\vec{b}_{sct}(s) = \mathbf{G}_{21}(s) \vec{b}_{int}(s) + \mathbf{G}_{22}(s) \vec{a}_{inc}(s) + \vec{y}_{sct}(s) \quad (13)$$

and replacing the internal quantities $\vec{b}_{int}(s)$ by the statement derived in Eq. 12 results in

$$\begin{aligned} \vec{b}_{sct}(s) = & \underbrace{\left[\mathbf{G}_{21}(s) [\mathbf{I} - \mathbf{G}_{11}(s)]^{-1} \right]}_{\mathbf{M}_{beam}(s) \in \mathbb{C}^{n \times m}} \vec{y}_{int}(s) + \vec{y}_{sct}(s) + \\ & \underbrace{\left[\mathbf{G}_{21}(s) [\mathbf{I} - \mathbf{G}_{11}(s)]^{-1} \mathbf{G}_{12}(s) + \mathbf{G}_{22}(s) \right]}_{\mathbf{S}_{csc}(s) \in \mathbb{C}^{n \times n}} \vec{a}_{inc}(s). \end{aligned} \quad (14)$$

The first two contributions of the sum reflect the influence of the beam driven signals of the substructures on the scattered waveguide port signals of the concatenated structure, whereas the last contribution gives the relationship between incident and scattered waveguide signals of the concatenated structure (common S-matrix description of full structure). Note, that it is impossible to compute the matrices $\mathbf{S}_{csc}(s)$ and $\mathbf{M}_{beam}(s)$ in general, since this implies the knowledge of the scattering properties $\mathbf{S}_k(s)$ of the individual segments on an infinite frequency interval. Nonetheless, these matrices can be computed in a finite frequency range, sampled at discrete frequencies, if the S-parameters of the segments are known in a finite frequency range, sampled at discrete frequencies. This frequency range may be adjusted by experimental needs.

As mentioned before, CSC does not consider beam excited signals. Since CTC is a generalization of CSC, the latter is included in Eq. 14, if the beam excited signals $\vec{y}_{int}(s)$ and $\vec{y}_{sct}(s)$ are set to zero, which means that no interaction between beam and structure takes place. In contrast, the focus of the presented method lies on the computation of beam driven port signals of large structures. In consequence, signals which are incident on that large structure are typically set to zero i.e. $\vec{a}_{inc}(s) = 0$.

Transfer to Time Domain

Due to the fact that the excitation of beam driven port signals is a transient process, Eq. 14 has to be transformed

into time domain. The complex quantities become real-valued and the multiplication becomes a convolution:

$$\vec{b}_{sct}(t) = \mathbf{M}_{beam}(t) * \vec{y}_{int}(t) + \vec{y}_{sct}(t). \quad (15)$$

From a signal processing point of view the equation above is the mathematical description of an analog filter. Its block diagram is sketched in Fig. 2. To avoid the direct evalua-

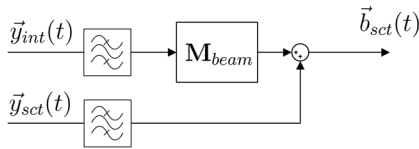


Figure 2: Block diagram of filter described in Eq. 15 with additional band-pass filters to bandlimit the input signals on a frequency interval, where the dynamic behaviour of the structure is described by $\mathbf{M}_{beam}(s)$.

tion of the convolution, a linear time-invariant system with multiple inputs and outputs is created by means of pole fitting [7], so that this system approximates the frequency domain behaviour of $\mathbf{M}_{beam}(s)$ (see Eq. 14) in a finite frequency range. The response of this system due to the stimulus $\vec{y}_{int}(t)$ is computed using standard ordinary differential equation solvers, whereas the final addition of this response to $\vec{y}_{sct}(t)$ to compute $\vec{b}_{sct}(t)$ is straightforward. It is spotlighted that the signals $\vec{y}_{int}(t)$ and $\vec{y}_{sct}(t)$ have to be filtered with a band-pass filter, such that these signals only contain frequencies on an interval, where $\mathbf{M}_{beam}(s)$ is determined.

PROOF OF CONCEPT

To show the validity of the presented method, the signal scattered in the right TM_{01} waveguide port of a chain of two cylindrical cavities (see Fig. 3), driven by an on-axis ultrarelativistic bunch with a length of $\sigma = 6$ mm and a total charge of $q = 1$ nC is considered. The reference sig-

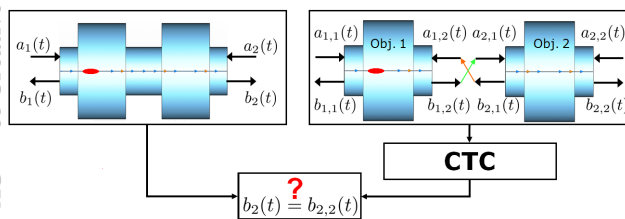


Figure 3: Comparison between direct computation vs. element-wise computation and concatenation using CTC.

nal $b_2(t)$ is computed by a straightforward wake field simulation of the entire structure performed by CST Particle SuiteTM [6]. The signal $b_{2,2}(t)$ is obtained by application of the CTC scheme, based on the S-parameters of the identical substructures, computed in the interval $\Delta f = 1 \dots 8$ GHz by CST's Fast S-parameter Solver [6] and the beam driven

port signals $\vec{y}_{int}(t)$ and $\vec{y}_{sct}(t)$ computed by CST Particle SuiteTM [6]. The beam driven port signals of obj. 2 are obtained by delaying the signals of obj. 1. Fig. 4 shows

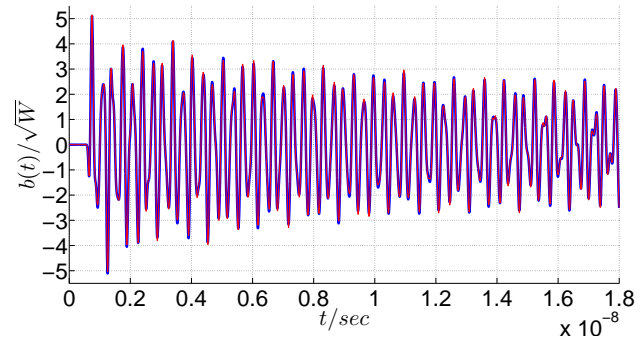


Figure 4: Comparison between direct computation $b_2(t)$ (blue curve) vs. element-wise computation of signal contributions and coupling using CTC $b_{2,2}(t)$ (red curve). The signals are filtered such that their band is restricted to Δf .

the proof of principle for the introduced method. It is observable that the beam driven port signal, acquired by the straightforward computation (blue plot) is almost identical to the signal obtained by element-wise computation followed by the CTC concatenation (red plot), although only the TM_{01} waveguide mode is contemplated for the cavity coupling. The absolute error in the two norm is given by

$$\frac{1}{N_s} \|b_2(kT) - b_{2,2}(kT)\|_2 = 8.9686 \cdot 10^{-4} \sqrt{W}, \quad (16)$$

where N_s is the total number of samples, T the constant time step size of the ODE solver and k the running index.

CONCLUSIONS

The presented method CTC enables the calculation of beam driven port signals of complex accelerator structures based on a priori computed S-parameters and transient wake field computations of the segments of the decomposed structure. Using this approach the computation of beam driven signals of large structures can be performed on standard hardware. It is important to note that the CTC formalism is not restricted to the simple monomodal setup, which is discussed in this paper, but is able to concatenate segments with more complex topologies. In particular multimodal coupling can be applied.

REFERENCES

- [1] H.-W. Glock et al., DIPAC2011, MOPD25
- [2] P. Zhang et al., DIPAC2011, MOPD17
- [3] K. Rothemund et al., TESLA-REPORT 2000-33
- [4] I.R.R. Shinton et al., IPAC 2010, WEPEC052
- [5] <http://www.slac.stanford.edu/grp/acd/t3p.html>
- [6] CST Studio SuiteTM, CST AG, 64289 Darmstadt, Germany.
- [7] B. Gustavsen et al., IEEE Trans. Power Delivery, vol. 14, no. 3, pp. 1052-1061, July 1999